

Support for the Lunar Cataclysm Hypothesis from Lunar Meteorite Impact Melt Ages

B. A. Cohen,*† T. D. Swindle, D. A. Kring

Lunar meteorites represent a more random sampling of lunar material than the Apollo or Luna collections and, as such, lunar meteorite impact melt ages are the most important data in nearly 30 years with which to reexamine the lunar cataclysm hypothesis. Within the lunar meteorite breccias MAC 88105, QUE 93069, DaG 262, and DaG 400, seven to nine different impact events are represented with ^{40}Ar - ^{39}Ar ages between 2.76 and 3.92 billion years ago (Ga). The lack of impact melt older than 3.92 Ga supports the concept of a short, intense period of bombardment in the Earth-moon system at ~ 3.9 Ga. This was an anomalous spike of impact activity on the otherwise declining impact-frequency curve.

In the early 1970s, ^{40}Ar - ^{39}Ar and U-Pb isotopic analyses of Apollo 15, 16, and 17 highland rocks (1, 2) revealed surprising, widespread isotopic disturbances at 3.9×10^9 years ago (Ga). Argon and lead losses (and correlated disturbances in the Rb-Sr system) were attributed to metamorphism of the lunar crust by an enormous number of asteroid and/or cometary collisions in a brief pulse of time [$<0.2 \times 10^9$ years (Gy)] in what was called the lunar cataclysm. This single event would have created the large basin structures and resurfaced much of the moon.

Subsequent high-precision ^{40}Ar - ^{39}Ar analyses of Apollo 14, 15, and 17 and Luna 24 impact melt rocks (3–7) indicated a range of ages, but none older than 4.0 Ga, supporting a cataclysm theory. However, the Apollo and Luna sample sites are restricted to the nearside equatorial region of the moon, within or near impact basins. Thus, the ages in these collections may be dominated by the Nectaris, Crisium, Serenitatis, and Imbrium impact events, which may obscure evidence of earlier events and may not reflect the global impact record on the moon.

Lunar meteorites, which were only recognized after the Apollo missions, provide a new opportunity to test the hypothesis. These are samples of the moon randomly ejected from the lunar surface (8) without enough velocity to escape the Earth-moon system. They experienced only mild shock during launch (9) and typically landed on Earth after $\sim 1 \times 10^6$ years (My) in space (9, 10). Meteorites that are chemically distinct from Apollo samples may not have been affected by nearside equatorial basin

impacts. Instead, impact melt clasts within these meteorites may have been formed in large-impact events in other regions of the moon (11).

We selected four lunar meteorites that are highlands regolith breccias, meaning they contain a variety of clasts from a few-kilometer area (9), including abundant impact melt (15 to 50% by volume). Two were collected in Antarctica (MAC 88105 and QUE 93069) and two in the Libyan desert (DaG 262 and DaG 400). Solar wind abundance measurements (12) show that DaG 262 and DaG 400 are not paired and, thus, were launched from the moon in different events. The cosmic-ray exposure (CRE) history of MAC 88105 (13, 14) distinguishes it from the other meteorites in this study, indicating a third launch event. Although QUE 93069 is similar to DaG 262 in chemistry and in CRE age, melt spherules are abundant in QUE 93069 and are lacking in DaG 262 (15), indicating their origins from different places on the moon.

Typical impact melt clasts were crystalline, fine-grained, microporphyratic, and plagioclase-rich. Their textures are similar to impact melt clasts identified in Apollo and Luna samples (16, 17), indicating their formation in relatively large impacts in which substantial amounts of melt were produced. In these large melt sheets, a slow cooling rate facilitates recrystallization and degassing. Although the textures of the lunar meteorite impact melt clasts are similar to those in the Apollo collection, their major element chemistry is quite different. The meteorite clasts are very anorthositic (An_{95-98}) and have, on average, 2 to 6 weight percent (wt%) less FeO and 1 wt% less TiO_2 than Apollo impact melts (17). In addition, the meteorite clasts contain ~ 0.01 wt% K_2O and <0.08 wt% P_2O_5 , elements that are abundant only in KREEP material [~ 1 wt% K_2O (K), rare earth elements

(REE), and ~ 0.1 wt% P_2O_5 (P)], which appears to be localized to the Procellarum region on the lunar nearside (18). The absence of this material in the meteorites indicates an origin on the east limb or farside.

Splits with masses ranging from 30 to 150 μg were extracted from melt clasts for ^{40}Ar - ^{39}Ar dating. After neutron irradiation, samples were step-heated with a continuous-wave laser (19). Of the 43 samples that were dated, 31 had interpretable ^{40}Ar - ^{39}Ar spectra. On the basis of the Ar release plateaus, isochrons, and K/Ca ratios of the data (after corrections for blanks, interferences, and cosmic-ray spallation), an age was computed for each sample (Table 1).

Each meteorite samples at least one distinct impact event, and at least seven different impact events are represented (Fig. 1 and Table 2). There is a distribution of separate events from 2.76 to 3.92 Ga, suggesting there was a large number of impacts before ~ 3 Ga. Although the existence of older impact melts with the data set cannot be ruled out, the data are consistent with a cataclysm. The simultaneous analysis of a 4.45-Ga clast from the H-chondrite Ourique (20) indicates that the ages are not artificially young because of systematic error in the data collection or reduction. The lack of impact melt ages older than 3.9 Ga is similar to the limit

Table 1. Impact melt clast ages (1σ uncertainty values are in parentheses). The extent of the Ar plateau is expressed by the percent of ^{39}Ar released in the plateau heating steps.

Sample	Age (Ga)	^{39}Ar (%)
MAC A	2.53 (1.50)	64
MAC B1	3.01 (0.17)	12
MAC C	3.35 (0.21)	82
MAC D	3.60 (0.27)	93
MAC F	3.81 (0.06)	29
MAC F2	3.94 (0.09)	47
MAC G	3.52 (0.33)	31
MAC H	3.91 (0.15)	77
MAC I	4.04 (0.10)	72
QUE E	3.85 (0.17)	44
QUE F	3.02 (0.42)	35
QUE G	2.52 (2.59)	52
QUE I	2.44 (1.85)	34
QUE K	4.01 (0.49)	36
262 H	4.12 (0.48)	61
262 Q2	3.55 (0.17)	51
262 R	2.43 (0.17)	54
400 A1	2.58 (0.35)	37
400 AA	3.10 (0.10)	49
400 BB	2.97 (0.08)	82
400 C1	2.51 (0.73)	27
400 C3	3.41 (0.09)	61
400 D	2.88 (0.52)	17
400 DD	3.11 (0.14)	48
400 FF	2.79 (0.27)	56
400 L9	2.46 (0.52)	100
400 L15	2.92 (0.19)	61
400 Q	3.47 (0.07)	64
400 T	3.34 (0.21)	64
400 T2	2.75 (0.37)	57
400 W	3.61 (0.04)	70

The University of Arizona, Tucson, AZ 85721, USA.

*Present address: Department of Geological Sciences, University of Tennessee, Knoxville, TN 37996, USA.

†To whom correspondence should be addressed. E-mail: bcohen@utk.edu

seen in the ages of Apollo impact melts, indicating that the intense bombardment recorded in the nearside equatorial region was a global phenomenon.

Some impact melt ages are younger than the 3.9-Ga cataclysmic event but have textures similar to melt rocks formed in large impacts (3, 4). There are ~300 craters with diameters 30 to 260 km that are stratigraphically post-Imbrian in age (21) which could have created these melts. Lunar spherules from the Apollo 14 site, which, because they cooled too quickly to recrystallize, may have been formed in even smaller impacts, have a similar age distribution (5). While impact melt older than 3.9 Ga is not present in these two data sets, very few young (<3.6 Ga) ages have been found for Apollo and Luna impact melt rocks, though they do exist (7). The sheer volume of impact melt created by the ~3.9-Ga basin-forming impacts may be bi-

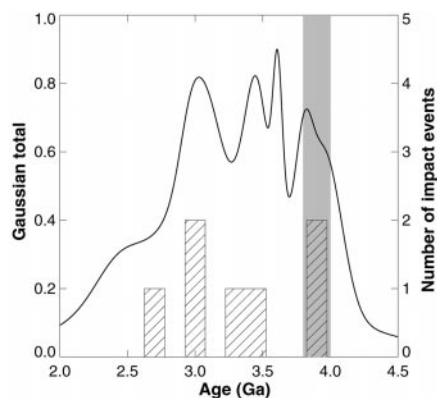


Fig. 1. Ideogram of impact melt ages. The ages of 31 impact melt clasts from these meteorites are represented as individual Gaussian distributions, where each Gaussian has a width proportional to the 1 σ age uncertainty and a unit area underneath it. The Gaussians are added together to produce a single curve and are re-normalized. The seven impact events in Table 2 are shown in the histogram (bin size, 0.20 Gy). The shaded area is a 0.20-Gy interval representing the lunar cataclysm. No impact melts within these meteorites predate the proposed cataclysm, though the sometimes large uncertainties produce a tail in the ideogram >3.9 Ga.

Table 2. Individual impact events. An impact event was defined as an age recorded by two or more clasts in a single meteorite. The age of each event (1 σ uncertainty values are in parentheses) was determined by fitting a normal distribution to the melt samples in the group.

Meteorite	Event (Ga)	No.
MAC 88105	3.35 (0.37)	5
MAC 88105	3.92 (0.14)	4
QUE 93069	3.00 (0.47)	3
QUE 93069	3.87 (0.23)	2
DaG 400	2.76 (0.38)	7
DaG 400	3.05 (0.13)	3
DaG 400	3.43 (0.10)	3

asing the sample age distribution in nearside melt rocks.

Correlation of Apollo samples with impact basin stratigraphy suggests that 80% of the lunar surface was resurfaced by craters and ejecta between the formation of the Nectaris and Orientale basins (21). This period of time was <0.2 Gy (2) and possibly was as brief as 0.02 Gy (22). Bombardment models based on the assumption of a steady falloff in the lunar cratering rate (23) predict a large number of impact melt samples older than 3.9 Ga. Other models (24, 25) to produce the observed impact melt distribution assume that isotopic resetting is easier and more widespread and that crustal pulverization is more extensive than experiments would suggest (26, 27). A “spike” in impactor flux at ~3.9 Ga (28) is the easiest way to match the impact melt age data.

The abundance of young impact melts and spherules might be explained by prolonged delivery of material from a catastrophic breakup event in the asteroid belt, though this may be dynamically unlikely at ~4 Ga (29). The distribution of ages suggests the bombardment may have lasted up to 0.5 Gy, as smaller debris was swept up by the moon following the larger basin forming events. Impact ages in eucrites, mesosiderites, and other meteorites have a similar distribution: none are older than ~3.9 Ga, with ages tailing down to 3.4 Ga or younger (30), suggesting the cataclysm affected the entire inner solar system, including Mars.

The cataclysm produced >1700 large (20 to 1200 km diameter) craters on the moon (21). The number of impacts occurring on Earth would have been at least an order of magnitude larger, implying >17,000 large impact events in a brief time. The largest of these probably produced immense quantities of ejecta, temporarily charged the atmosphere with silicate vapor, and boiled away large quantities of surface water (31). Coincidentally, the earliest isotopic evidence of life on Earth is also ~3.9 Ga (32). If a swarm of impactors at 3.9 Ga returned the surface of Earth to a hot and energetic state, the rise or evolution of life on Earth would have been affected. The effect may have been detrimental, by destroying existing life or organic fragments (33), or beneficial, by delivering precursor molecules (34) and providing suitable environments for evolution (35). Either way, a catastrophic bombardment of the Earth-moon system affected the origin and evolution of life.

References and Notes

- G. Turner, P. H. Cadogan, C. J. Yonge, *Proc. Lunar Planet. Sci. Conf.* **4**, 1889 (1973).
- F. Tera, D. A. Papanastassiou, G. J. Wasserburg, *Earth Planet. Sci. Lett.* **22**, 1 (1974).
- G. B. Dalrymple, G. Ryder, *J. Geophys. Res.* **98**, 13085 (1993).

- _____, *J. Geophys. Res.* **101**, 26069 (1996).
- T. S. Culler, T. A. Becker, R. A. Muller, P. R. Renne, *Science* **287**, 1785 (2000).
- P. H. Cadogan, G. Turner, *Philos. Trans. R. Soc. London Ser. A* **284**, 167 (1977).
- T. D. Swindle, P. D. Spudis, G. J. Taylor, R. L. Korotev, J. R. H. Nichols, *Proc. Lunar Planet. Sci. Conf.* **21**, 167 (1990).
- P. H. Warren, G. W. Kallemeyn, *Geochim. Cosmochim. Acta* **55**, 3123 (1991).
- P. H. Warren, *Icarus* **111**, 338 (1994).
- B. J. Gladman, J. A. Burns, M. Duncan, H. Levison, *Icarus* **118**, 302 (1995).
- G. J. Taylor, *Geochim. Cosmochim. Acta* **55**, 3031 (1991).
- P. Scherer, M. Pätzsch, L. Schultz, *Meteorit. Planet. Sci.* **33**, A135 (1998).
- K. Nishizumi et al., *Geochim. Cosmochim. Acta* **55**, 3149 (1991).
- O. Eugster et al., *Geochim. Cosmochim. Acta* **55**, 3139 (1991).
- A. Bischoff et al., *Meteorit. Planet. Sci.* **33**, 1243 (1998).
- D. A. Stöffler et al., *J. Geophys. Res.* **90**, C449 (1985).
- G. J. Taylor et al., in *Lunar Sourcebook*, G. H. Heiken, D. T. Vaniman, B. M. French, Eds. (Cambridge Univ. Press, New York, 1991), pp. 183–284.
- B. L. Jolliff, J. J. Gillis, L. A. Haskin, R. L. Korotev, M. A. Wieczorek, *J. Geophys. Res.* **105**, 4197 (2000).
- Samples were irradiated in high-purity aluminum holders for 500 hours at the University of Michigan, producing a J-factor of 7.33×10^{-2} . K_2SO_4 and CaF_2 salts were irradiated simultaneously to correct for reactor-induced interferences, Ga1550 biotite was used to derive the neutron fluence, and MMHb-1 hornblende was used as a check. The calculated ages for three aliquots of MMHb-1 were 523.6 ± 8.2 , 523.3 ± 9.9 , and 526.4 ± 10.3 Ma (1 σ errors), consistent with the published value of 523.1 ± 2.6 Ma (36). A continuous-wave laser system was used to step-heat 43 samples in three to nine steps, and a VG5400 mass spectrometer was used to collect the Ar gas. In addition to normal blank and interference corrections, Ar produced by cosmic-ray spallation was subtracted from each sample by deconvolving the proportion of ^{36}Ar from cosmic-ray spallation ($^{38}Ar/^{36}Ar = 1.5$) (36) and from terrestrial atmosphere and/or lunar Ar ($^{38}Ar/^{36}Ar = 0.19$) (37, 38). This procedure often entirely corrected for ^{36}Ar . Isochron diagrams to constrain the initial $^{40}Ar/^{36}Ar$ usually did not have good correlations; however, in those that did have good correlations, the initial $^{40}Ar/^{36}Ar$ was <0.1, indicating a negligible contribution from the solar wind. In about five samples, a full terrestrial atmosphere ($^{40}Ar/^{36}Ar = 295.5$) could be subtracted from the data. The apparent ages derived after this subtraction were identical to the apparent sample age without this extreme correction. Even in samples containing an uncorrected amount of ^{40}Ar , the apparent ages will be older than, not younger than, the true ages. This effect is irrelevant to our conclusions. Representative plateau and isochron data can be found at Science Online at www.sciencemag.org/cgi/content/full/290/5497/1754/DC1. Further details of data collection and reduction may be found in (39).
- D. A. Kring, B. A. Cohen, T. D. Swindle, D. H. Hill, in *Lunar and Planetary Science* (Lunar and Planetary Institute, Houston, 2000), vol. XXXI, abstract #1688, available on CD-ROM.
- D. E. Wilhelms, *U.S. Geol. Surv. Prof. Pap.* **1348** (1987).
- G. Ryder, *Eos* **81**, S76 (2000).
- W. K. Hartmann, *Icarus* **24**, 181 (1975).
- D. H. Grinspoon, thesis, University of Arizona (1989).
- J. B. Hartung, *Meteoritics* **9**, 349 (1974).
- L. E. Nyquist, C.-Y. Shih, *Geochim. Cosmochim. Acta* **56**, 2213 (1992).
- A. Deutsch, U. Schärer, *Meteoritics* **29**, 301 (1994).
- G. Turner, *Proc. Lunar Planet. Sci. Conf.* **10**, 1917 (1979).
- V. Zappala, A. Cellino, B. J. Gladman, S. Manley, F. Migliorini, *Icarus* **134**, 176 (1998).
- D. D. Bogard, *Meteoritics* **30**, 244 (1995).

31. N. H. Sleep, K. Zahnle, *J. Geophys. Res.* **103**, 28529 (1998).
32. S. J. Mojzsis, T. M. Harrison, *GSA Today* **10**, 1 (April 2000).
33. N. H. Sleep, K. J. Zahnle, J. F. Kasting, H. J. Morowitz, *Nature* **342**, 139 (1989).
34. E. Pierazzo, C. F. Chyba, *Meteorit. Planet. Sci.* **34**, 909 (1999).
35. D. A. Kring, *GSA Today* **10**, 1 (August 2000).
36. P. R. Renne *et al.*, *Chem. Geol.* **145**, 117 (1998).
37. C. M. Hohenberg, K. Marti, F. A. Podosek, R. C. Reedy, J. R. Shirck, *Proc. Lunar Planet. Sci. Conf.* **9**, 2311 (1978).
38. T. D. Swindle, in *Meteorites and the Early Solar System* J. F. Kerridge, M. S. Matthews, Eds. (Univ. of Arizona Press, Tucson, 1988), pp. 535–564.
39. B. A. Cohen, thesis, University of Arizona (2000).
40. We thank A. Bischoff and J. Zipfel for providing us with DaG 262 and DaG 400. L. Dones and an anonymous reviewer provided constructive reviews. This research was supported with a NASA Space Grant Fellowship (B.A.C.) and by NAG5-4944 (D.A.K.) and NAG5-4767 (T.D.S.) and used the NASA Astrophysical Data System Abstract Service.

22 August 2000; accepted 20 October 2000

Nitric Acid Trihydrate (NAT) in Polar Stratospheric Clouds

Christiane Voigt,¹ Jochen Schreiner,¹ Andreas Kohlmann,¹
 Peter Zink,¹ Konrad Mauersberger,^{1*} Niels Larsen,²
 Terry Deshler,³ Chris Kröger,³ Jim Rosen,³ Alberto Adriani,⁴
 Francesco Cairo,⁴ Guido Di Donfrancesco,⁴ Maurizio Viterbini,⁴
 Joelle Ovarlez,⁵ Henri Ovarlez,⁵ Christine David,⁶
 Andreas Dörnbrack⁷

A comprehensive investigation of polar stratospheric clouds was performed on 25 January 2000 with instruments onboard a balloon gondola flown from Kiruna, Sweden. Cloud layers were repeatedly encountered at altitudes between 20 and 24 kilometers over a wide range of atmospheric temperatures (185 to 197 kelvin). Particle composition analysis showed that a large fraction of the cloud layers was composed of nitric acid trihydrate (NAT) particles, containing water and nitric acid at a molar ratio of 3:1; this confirmed that these long-sought solid crystals exist well above ice formation temperatures. The presence of NAT particles enhances the potential for chlorine activation with subsequent ozone destruction in polar regions, particularly in early and late winter.

Since the early 1980s, the formation of a large ozone hole above Antarctica during southern spring has become a yearly event. Stratospheric air isolated within the polar vortex cools during winter to temperatures that allow the formation of polar stratospheric clouds (PSCs) at altitudes between 15 and 25 km (1). The cloud particles provide surfaces for the activation of otherwise relatively unreactive chlorine-containing molecules. Upon the return of sunlight in the spring, the cloud-processed chlorine species are photolyzed and induce dramatic ozone losses (2). To a lesser extent, the north polar stratosphere also experiences low winter temperatures within a well-developed vortex, leading to the formation of PSCs and subsequent ozone destruction (3). Satellite and field measurements in both polar

regions have shown that many PSCs exist well above the frost point of water, T_{ICE} , the temperature in the stratosphere near 188 K below which ice particles can form (4–6). For those PSCs the important role of the trace gas nitric acid (HNO_3) has been recognized. Early atmospheric models predicted the formation of solid nitric acid hydrate crystals at temperatures above T_{ICE} (7, 8). Laboratory studies revealed that nitric acid trihydrate (NAT, $\text{HNO}_3 \cdot 3\text{H}_2\text{O}$) would be stable up to 7° above the frost point in the lower stratosphere (9). Measurements at these temperatures from high-flying aircraft and ground-based LIDAR (light detection and ranging), however, often identified liquid supercooled ternary solution (STS) droplets instead of solid particles (10–12).

The composition, phase, and formation temperature range of PSCs are critical for atmospheric models that predict ozone losses in polar regions. NAT is believed to be the most stable particle under stratospheric conditions. As a result of its low vapor pressure, NAT can exist at higher temperatures than STS droplets or ice particles, with the consequence that chlorine activation can proceed over wider areas and for longer time periods. By scavenging nitrogen compounds, NAT particles hinder the passivation of active chlorinated substances through reactions with nitrogen oxides. The removal of particles through sedimentation to lower altitudes, a process called denitrification, increases the efficiency of chlorine activation

and is only possible through the formation of crystalline PSC particles. Despite their importance, no direct chemical analysis of NAT particles in the stratosphere has been made, although they have been identified in many laboratory studies (9, 13) and inferred from atmospheric measurements (6).

In January 1998, a direct particle composition measurement was performed in lee wave-induced PSCs above Scandinavia (14–16). STS droplets containing water, nitric acid, and sulfuric acid were observed. As expected from STS theory, a close correlation between low atmospheric temperatures and the presence of PSCs was found. A more comprehensive set of instruments to investigate chemical, physical, and optical properties of PSCs was launched at 20 UT (universal time) on 25 January 2000 from the balloon facility Esrange, near Kiruna, Sweden. The crucial instrument on both flights was an aerosol composition mass spectrometer (ACMS) that uses an aerodynamic lens to focus particles into a narrow beam (17) and separates them from ambient gases. The particles are then evaporated inside a small sphere, and the evolving gases are analyzed with a mass spectrometer. Simultaneous measurements of particle number density and size were performed with particle counters (18, 19). Backscatter ratios and depolarization were measured with two backscatter sondes (20, 21). A water vapor experiment determined the frost point T_{ICE} (22). A number of sensors measured the ambient stratospheric temperature with a precision better than ± 0.5 K to establish a correlation with PSC particle parameters such as volume and composition.

A vertical cross section of the temperature distribution along the flight track at 22 UT was simulated with a mesoscale meteorological model (23) (Fig. 1). The balloon trajectory (thick line) crosses the extension of a cold trough that had developed over the Scandinavian mountains as a result of adiabatic expansion of ascending air masses in mountain-induced gravity waves. Temperatures determined during the flight are in general agreement with the model simulations, although the latter cannot resolve the measured small-scale temperature fluctuations. The cold temperature pattern between 21 and 24 km extended upwind toward the Scandinavian mountains, indicating that particles sampled during the flight could have nucleated in those cold regions. Near 22 km on the first ascent, the observed temperatures were 1 to 2 K below T_{ICE} . During the 2-hour mea-

¹Max-Planck-Institut für Kernphysik, Division of Atmospheric Physics, Post Office Box 103 980, D-69029 Heidelberg, Germany. ²Division of Middle Atmosphere Research, Danish Meteorological Institute, Lyngbyvej 100, DK-2100 Copenhagen, Denmark. ³Department of Atmospheric Science, University of Wyoming, Post Office Box 3038, Laramie, WY 82071, USA. ⁴CNR-Istituto di Fisica dell'Atmosfera, Via Fosso del Cavaliere 100, I-00133 Rome, Italy. ⁵Laboratoire de Météorologie Dynamique du CNRS, École Polytechnique, F-91128 Palaiseau, France. ⁶Service d'Aéronomie du CNRS, Institut Pierre-Simon Laplace, Université Paris, 4 place Jussieu, F-75252 Paris, France. ⁷DLR Oberpfaffenhofen, Institut für Physik der Atmosphäre, D-82234 Wessling, Germany.

*To whom correspondence should be addressed. E-mail: Konrad.Mauersberger@mpi-hd.mpg.de